

**CUTTINGTOOLS2024-00008**

## **THE INFLUENCE OF CUTTING EDGE RADIUS, CUTTING SPEED AND FEED ON SURFACE ROUGHNESS AND MICROHARDNESS IN MACHINING STAINLESS STEEL**

T. Vopat<sup>1\*</sup>, K. Bartova<sup>2</sup>, M. Domankova<sup>2</sup>, S. Lenghart<sup>1</sup>, D. Zajko<sup>1</sup>

<sup>1</sup>Slovak University of Technology in Bratislava, Faculty of Materials Science and Technology in Trnava, Institute of Production Technologies, Jana Bottu 25, 917 24 Trnava, Slovak Republic

<sup>2</sup>Slovak University of Technology in Bratislava, Faculty of Materials Science and Technology in Trnava, Institute of Materials Science, Jana Bottu 25, 917 24 Trnava, Slovak Republic

\*Corresponding author; e-mail: [tomas.vopat@stuba.sk](mailto:tomas.vopat@stuba.sk)

### **Abstract**

The article investigates the impact of cutting edge radius and cutting parameters on the surface roughness and microhardness of austenitic stainless steel (AISI 321) during external turning. Experiment was performed for cemented carbide cutting inserts with cutting edge radii of 5  $\mu\text{m}$ , 18  $\mu\text{m}$ , and 50  $\mu\text{m}$ . Cutting edge with radius size of 5  $\mu\text{m}$  had sharp cutting edges containing small chamfers and burrs of approximately 5  $\mu\text{m}$  in size. Cutting speed and feed were varied in the experiment. Surface roughness parameters ( $R_a$ ,  $R_z$ ) and microhardness (HV) were measured. The results indicate that feed and cutting edge radius significantly influence surface roughness, while cutting speed has minimal effect. Microhardness increases with larger cutting edge radii due to strain hardening caused by material deformation beneath the cutting tool. ANOVA analysis confirmed that the interaction between feed and cutting edge radius plays a crucial role in determining the final surface quality. These findings provide insights into optimizing machining parameters for improved surface integrity and mechanical properties in stainless steel turning.

### **Keywords:**

Cutting edge radius, Work hardening, Strain hardening, Microhardness, Edge preparation

## **1 INTRODUCTION**

Strain hardening, also known as work hardening, refers to the phenomenon where a material's hardness and strength increase due to plastic deformation during processes such as machining.

The cutting edge radius plays a crucial role in determining the extent of strain hardening in the machined surface [Filippov 2020] when milling aluminium alloy. A larger cutting edge radius can lead to increased contact between the tool and the workpiece, resulting in greater plastic deformation and, consequently, a higher degree of strain hardening. Conversely, a smaller cutting edge radius may reduce the contact area, leading to less deformation and a softer machined surface. Cutting parameters, including cutting speed, feed, and depth of cut, significantly influence the strain hardening effect. Higher feed values and depths of cut can enhance the mechanical deformation of the material, promoting greater strain hardening [Hua 2018].

Sharman et al. [Sharman 2004] conducted turning experiments on Inconel 718 to evaluate the surface integrity of machined components. Their findings indicated that the feed was the primary factor affecting surface roughness, with higher feed values leading to increased roughness. In

contrast, the cutting speed had minimal influence on the surface roughness of the machined parts.

However, it is necessary to state that there is a difference between stable and unstable machining conditions. The results indicate that reducing the cutting speed enhances the surface quality of turned holes. However, it is important to note that this observation cannot be generalized to all machining processes. Instead, it specifically applies to internal turning using small-diameter boring bars, where unstable cutting conditions pose a challenge. Higher cutting speeds tend to decrease the stability of the cutting process [Vopat 2024].

Pawade et al. [Pawade 2008] examined the impact of machining parameters and cutting edge geometry on the surface integrity of high-speed turned Inconel 718. Their study revealed that the extent of work hardening beneath the subsurface was significantly affected by the cutting edge geometry and the depth of cut. However, the influence of cutting speed on work hardening was not clearly evident.

The work hardening behaviour was affected by the chamfer edge micro-geometry. Increasing both the chamfer width and chamfer angle can enhance work hardening. Additionally, the depth of the hardened layer increased with

increasing feed (the uncut chip thickness) in orthogonal cutting. However, the maximum microhardness on the machined surface did not exhibit significant differences [Zhou 2022].

In the article [Vopát 2020], the effect of cutting edge radius sizes on tool life during the turning of austenitic stainless steel was investigated. The results indicated that cemented carbide turning inserts with a larger cutting edge radius experienced faster tool wear during machining. This accelerated wear can be attributed to strain hardening. A larger cutting edge radius intensified strain hardening, leading to a harder machined surface.

Research has demonstrated that tool wear has a significant impact on surface integrity, including surface roughness and strain hardening. To eliminate the influence of tool wear in this study, each turning experiment was performed using a new cutting tool [Bushlya 2014]. For this reason, each sample was machined using new cutting insert in the experiment.

In this article, the influence of cutting conditions such as cutting speed, feed, and cutting edge radius on the surface roughness and microhardness of the machined surface was determined. Additionally, investigating the combined effect of individual cutting conditions in the machining process is of particular interest.

## 2 MATERIALS AND METHODS

The experiment examined the influence of cutting edge radius sizes and cutting parameters on selected aspects of machining stainless steel material using external turning. The aim of the experiment was to investigate the effect of cutting edge radius size, as well as the combination of cutting parameters and cutting edge radius size, on the surface roughness and microhardness of the strain-hardened top layer.

### 2.1 Selected cutting tools and workpiece material

The workpiece material used in the experiment was austenitic stainless steel, specifically DIN EN X6CrNiTi18-10 (AISI 321). Its chemical composition is presented in Tab. 1. The cutting tests were performed on a round bar with a diameter of 40 mm.

Tab. 1: Chemical composition of machined material DIN EN X6CrNiTi18-10 (AISI 321) grade.

Elem.	C	Si	Mn	P	S	Cu	Cr	Ni	Mo	Ti
wt. %	0,64	0,83	1,44	0,02	0,02	0,66	17,5	9,89	0,46	0,47

CNMG 120408 cemented carbide cutting inserts (WC+Co10%) were used as samples in the experimental research. These inserts, supplied by the Dormer Pramet tool company, are commonly used for turning applications. The manufactured cemented carbide cutting inserts had the following dimensions:

- Length of cutting edge: 12.9 mm
- Thickness: 4.76 mm
- Apex angle between cutting edge: 80°
- Diameter of centre hole for clamping system: 5.16 mm
- Nose radius:  $r_n$  0.8 mm
- Cutting edge radius  $r_\beta$ : 5  $\mu\text{m}$ , 18  $\mu\text{m}$ , 50  $\mu\text{m}$

Specific cutting edge radius sizes with values of 18 – 50  $\mu\text{m}$  were prepared by drag finishing, whereas a cutting edge radius of 5  $\mu\text{m}$  was not prepared. These radii had sharp

cutting edges containing small chamfers and burrs of approximately 5  $\mu\text{m}$  in size. For this experiment, a PCLNL 2020K12 tool holder was selected.

### 2.2 Cutting tests

In the experiment, a total of 18 trials were conducted. The cutting edge radius was adjusted at three different levels. Among the cutting parameters, the cutting speed was varied at two levels, while the feed was adjusted at three levels. The depth of cut remained constant throughout the experiment. The cutting conditions used in the experiment are presented in Tab. 2.

Tab. 2: Cutting conditions.

Input parameter (factors)	Level 1	Level 2	Level 3
Cutting edge radius $r_\beta$ ( $\mu\text{m}$ )	5 (sharp)	18	50
Feed $f$ (mm)	0.12	0.2	0.3
Cutting speed $v_c$ ( $\text{m} \cdot \text{min}^{-1}$ )	100	250	

For the cutting tests, the DMG CTX alpha 500 turning centre was used. A water-based emulsion with a 5% oil concentration was used as a coolant. A total of 18 samples were prepared from the workpiece material, and surface roughness parameters ( $R_a$  and  $R_z$ ) as well as microhardness (HV) were measured. A drawing of the sample, along with an explanation of the area of measurements, is shown in Fig. 1.

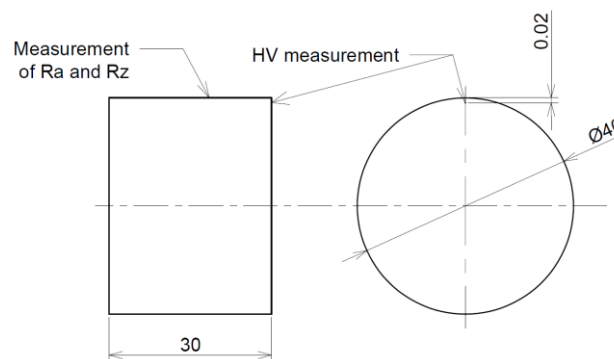


Fig. 1: Scheme of a sample for surface roughness and HV measurements (dimensions in mm).

### 2.3 Measurement of surface roughness

After the cutting tests, the surface roughness parameters  $R_a$  and  $R_z$  of the machined surface were evaluated. In the experiment, these parameters were measured using the Mitutoyo Surftest SJ-210 surface roughness measuring instrument. Each sample's machined surface was tested three times to obtain  $R_a$  and  $R_z$  values, after which the average value was calculated.

### 2.4 Measurement of microhardness of the strain-hardened top layer

Microhardness was measured using Hanemann's method, which employs a Vickers pyramid-shaped indenter mounted in a special lens. The evaluation was performed using the Neophot 21 device. A loading force of 0.1 kp for a 10-second load time was applied during measurement. Microhardness was measured on cross-sections near the turned surface (approximately 20  $\mu\text{m}$  below the surface). To obtain the average value, 10 measurements were performed on each sample, and the standard deviation was then calculated.

### 3 RESULTS

The results include an experimental and statistical analysis evaluating the influence of cutting edge radius sizes and cutting parameters on the surface roughness parameters Ra and Rz, as well as the microhardness of the strain-hardened top layer in machining stainless steel material.

#### 3.1 Surface roughness

The graphs of the average values of Ra and Rz with respect to the cutting edge radius sizes, cutting speed, and feed were plotted, as seen in Fig. 2 and Fig. 3. The smallest Ra value of 2.607  $\mu\text{m}$  and Rz value of 0.499  $\mu\text{m}$  were reached for a cutting edge radius size of 5  $\mu\text{m}$  (sharp cutting edge) and a feed value of 0.12 mm. The largest Ra value of 3.764  $\mu\text{m}$  and Rz value of 15.904  $\mu\text{m}$  were reached for a cutting edge radius size of 5  $\mu\text{m}$  (sharp cutting edge) and a feed value of 0.3 mm. Cutting speed was not a significant factor, as only minimal changes in Ra and Rz values were observed.

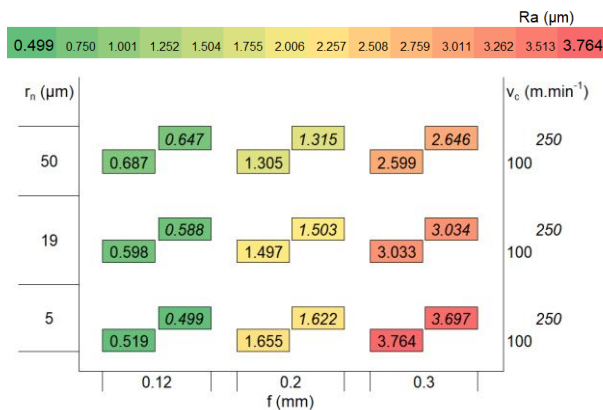


Fig. 2: Graph of Ra ( $\mu\text{m}$ ) with respect to the cutting edge radius size, cutting speed, and feed.

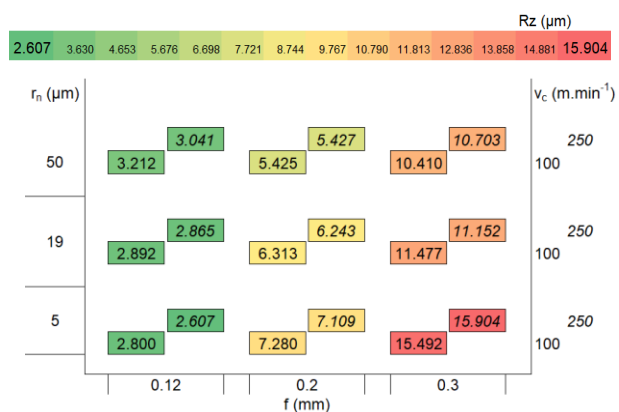


Fig. 3: Graph of Rz ( $\mu\text{m}$ ) with respect to the cutting edge radius size, cutting speed, and feed.

It can be seen from the graphs that surface roughness was affected by input parameters. It is noticeable how specific levels of input parameters such as cutting edge radius and feed impact the values of Ra and Rz. If cutting speed values were varied from 100 to 250  $\text{m}\cdot\text{min}^{-1}$ , no significant change in surface roughness occurred.

The ANOVA analysis results for Ra and Rz indicate that the observed input parameters (factors), such as cutting edge radius and feed, and their interactions ( $r_\beta * f$ ) had a significant influence on the measured responses (Ra and Rz). This is confirmed by the P-values. However, cutting speed and other individual interactions between process parameters were not statistically significant, as their p-

values exceeded 0.05. The overall predictive value of the model was determined based on the adjusted coefficient of multiple determination ( $R^2$ ). The results for Ra and Rz are presented in Tab. 3.

Tab. 3: ANOVA analysis for Ra and Rz.

Source	Degrees of freedom	Ra	Rz
		P-value	P-value
Model	13	0.000*	0.000*
$r_\beta$	2	0.000*	0.000*
$f$	2	0.000*	0.000*
$v_c$	1	0.578	0.771
$r_\beta * f$	4	0.000*	0.000*
$r_\beta * v_c$	2	0.566	0.690
$f * v_c$	2	0.618	0.519
adj. $R^2$ (only statistically significant factors)		99.96%	99.86%

\* denotes statistically significant model terms

The graphs in Fig. 4 and Fig. 5 display plots for all main effects. Analysing these graphs aids in interpreting and enhancing the understanding of a crucial aspect of the ANOVA results, particularly regarding the influence of the main input parameters on the studied variables (Ra and Rz). In this model, the surface roughness parameters Ra and Rz are significantly influenced by cutting edge radius size and feed. Cutting speed has no significant effect on changing surface roughness.

The change in surface roughness parameters Ra and Rz is most affected by feed within the studied parameter range. The curve of dependence of Ra and Rz on feed has the steepest gradient. In the case of feed, it is necessary to consider the well-known fact that by copying the shape of the nose radius into the machined surface, surface roughness deteriorates at higher feed values [Brown 2020], [Petropoulos 1973], [Shah 2020].

Therefore, it is possible to observe an increase in Ra and Rz values with increasing feed, as expected.

For cutting edge radius, it is necessary to investigate the range of speed values and its interaction with other cutting parameters. However, it cannot be stated that increasing cutting edge radius size consistently decreases Ra and Rz, as seen in the graph of Ra and Rz dependence on cutting edge radius. This brings only a general evaluation for the selected range of input parameters. For this reason, results should be evaluated based on the complete analysis, where values of cutting edge radius and feed influence each other (Fig. 6 and Fig. 7.).

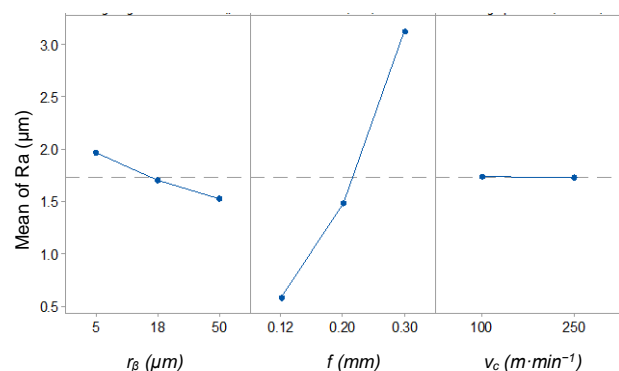


Fig. 4: Graph of the effects of the input parameters on Ra.

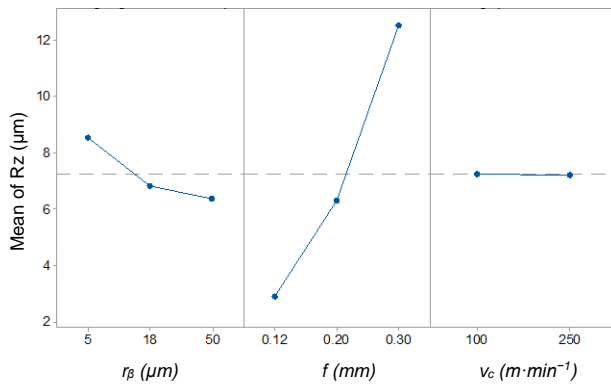


Fig. 5: Graph of the effects of the input parameters on Rz.

Therefore, it is necessary to analyse the interaction between the cutting edge radius and the feed, as seen from the graphs in Fig. 6 and Fig. 7. For the feed value of 0.3 mm, with increasing cutting edge radius size, the Ra and Rz values significantly decrease. A similar case applies for a feed value of 0.2 mm, with increasing cutting edge radius size, the Ra and Rz values decrease, but this decreasing tendency is not so significant as with a feed value of 0.3 mm. The opposite trend was observed for a feed value of 0.12 mm. With increasing cutting edge radius size, the Ra and Rz values increase. It brings novel findings.

Authors assumed that it is related to the cutting process and the ratio of the uncut thickness and cutting edge radius size. This is followed by the results of the strain hardening of the top layer. The detailed analysis is stated in the Discussion.

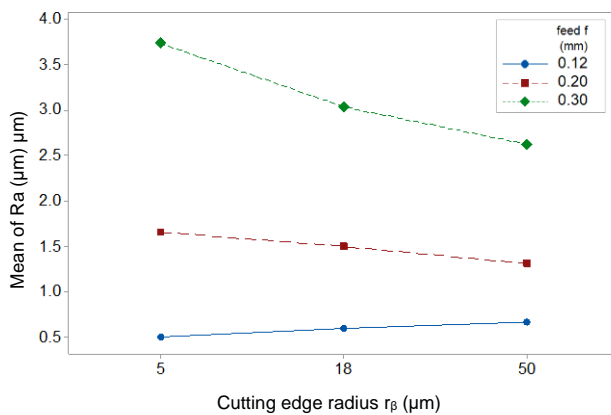


Fig. 6: Graph of the interaction plot for Ra.

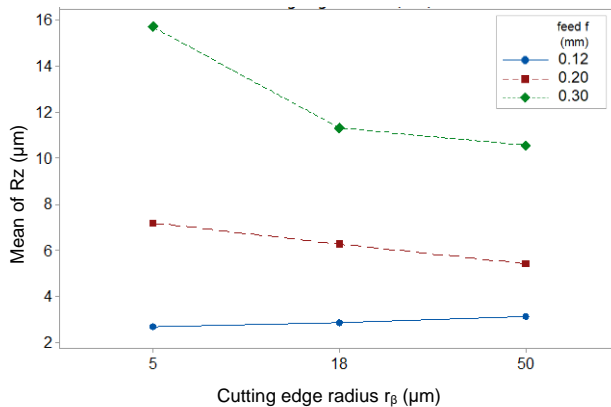


Fig. 7: Graph of the interaction plot for Rz.

### 3.2 Microhardness of the strain-hardened top layer

The microhardness values of workpiece material that was not affected by machining were approximately 280 HV.

The ANOVA analysis results for microhardness indicate that cutting edge radius had a significant influence on the measured microhardness (HV). However, feed, cutting speed, and individual interactions between process parameters were not statistically significant, as their p-values exceeded 0.05. The overall predictive value of the model was determined based on the adjusted coefficient of multiple determination ( $R^2$ ). The results for microhardness (HV) are presented in Tab. 4.

Tab. 4: ANOVA analysis for microhardness.

Microhardness		
Source	Degrees of freedom	P-value
<b>Model</b>	13	0.017*
$r_\beta$	2	0.001*
$f$	2	0.363
$v_c$	1	0.337
$r_\beta * f$	4	0.242
$r_\beta * v_c$	2	0.632
$f * v_c$	2	0.480
<b>adj. <math>R^2</math></b> (only statistically significant factors)		84.81%

\* denotes statistically significant model terms

The graph of the average values of microhardness (HV) with respect to the cutting edge radius sizes, cutting speed, and feed was plotted, as seen in Fig. 8

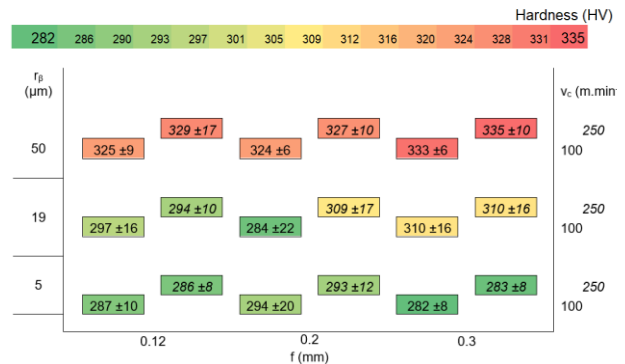


Fig. 8: Graph of microhardness values (HV) with respect to the cutting edge radius size, cutting speed, and feed.

The graph illustrates how particular cutting edge radius values impact the microhardness of the top layer, where significant changes in HV values occurred. The smallest microhardness value of 282 HV was observed for a cutting edge radius size of 5 μm (sharp cutting edge), indicating that the top layer of the machined surface was minimally affected by the cutting edge radius. The largest microhardness value of 335 HV was reached for a cutting edge radius size of 50 μm, demonstrating the strongest effect of strain hardening on the top layer after machining. The cutting speed and feed were not significant factors, as the variations in HV values were similar to measurement deviations. The graph in Fig. 9 displays the plot for all main effects.

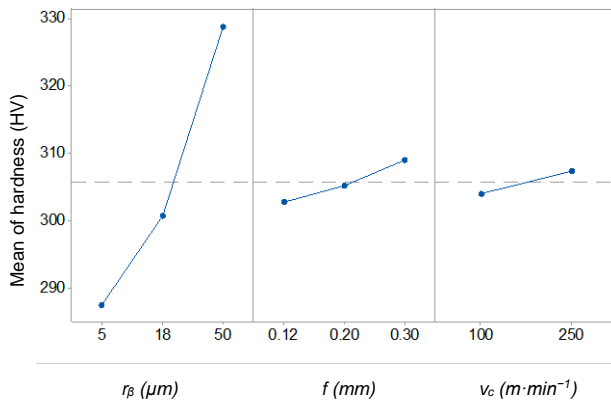


Fig. 9: Graph of the effects of the input parameters on microhardness (HV).

The change in microhardness is most affected by the cutting edge radius size, where the dependence of hardness (HV) on cutting edge radius has the steepest curve. This is related to the cutting zone, where a certain thickness of workpiece material is not cut but instead pressed. As a result, the newly machined surface becomes significantly harder than the original work surface. A detailed analysis is presented in the Discussion.

The use of a cutting tool with a cutting edge radius size of 50  $\mu\text{m}$  led to an approximately 20% increase in microhardness in the top layer after machining due to strain hardening. The curves of other individual dependencies exhibit only moderate variations, confirming their statistical insignificance from the ANOVA analysis.

## 4 DISCUSSION

The results were analysed during the machining of austenitic stainless steel, which exhibits a high strain-hardening tendency. For this reason, strain hardening plays a crucial role in the obtained results. Strain hardening is related to the separation (stagnation) point. The position of the separation point can be influenced by various factors. Rodríguez in publication [Rodríguez 2009] proposed a model that describes the relationship among the minimum uncut chip thickness ( $h_{\min}$ ), friction angle, cutting edge radius ( $r_\beta$ ), and other parameters. The concept of separation point in the cutting zone (inspired by [Rodríguez 2009]) is shown in Fig. 10.

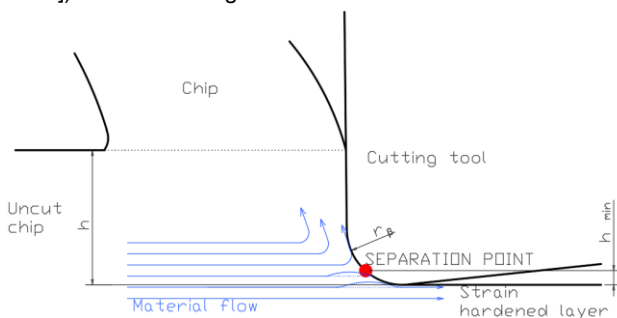


Fig. 10: Concept of separation point in the cutting zone.

Above this separation point S, the material is assumed to flow into the chip and be cut. Below the separation point, the material is pressed by the cutting tool and flows into the newly machined surface. This thickness of the workpiece represents the minimum uncut chip thickness ( $h_{\min}$ ), causing strain hardening of the machined surface, which directly increases the microhardness of the top layer.

In the case of microhardness, if the cutting edge radius is larger, the minimum uncut chip thickness also increases because the separation point is positioned higher in accordance with this model. This means that a larger uncut chip thickness (i.e., a larger amount of workpiece material) is pressed by the cutting edge, resulting in increased microhardness of the top layer, as seen in Fig. 8 and Fig. 9.

This statement can also be applied to the resulting surface quality. Since the material is pressed below the separation point, the force required to press the material with the cutting tool increases. Authors in publication [Boothroyd 2006] describe this force as ploughing or ploughing force. The ploughing force depends on the cutting edge radius, which increases the resultant force in machining.

The authors assumed that the existence of ploughing force affects machining stability, which can be reflected in the deterioration of surface roughness. However, it is not necessarily true that avoiding ploughing force (i.e., using a sharp cutting edge) results in better surface roughness. The experimental results showed that the ratio of the cutting edge radius to the uncut thickness ( $r_\beta/h$ ) is crucial. In orthogonal turning, the uncut chip thickness is equal to the feed when the side cutting angle is 90°. Therefore, if the side cutting angle is about 90° (as it was 95° in this experiment), it is possible to consider the ratio of feed (instead of uncut chip thickness  $h$ ) and cutting edge radius.

After analysing the results, the extreme values were reached for the sharp cutting edge (5  $\mu\text{m}$ ), where the lowest Ra value (0.499  $\mu\text{m}$ ) was measured for a feed value of 0.12 mm, and the highest Ra value (3.764  $\mu\text{m}$ ) was measured for a feed value of 0.3 mm, as shown in Fig. 11.

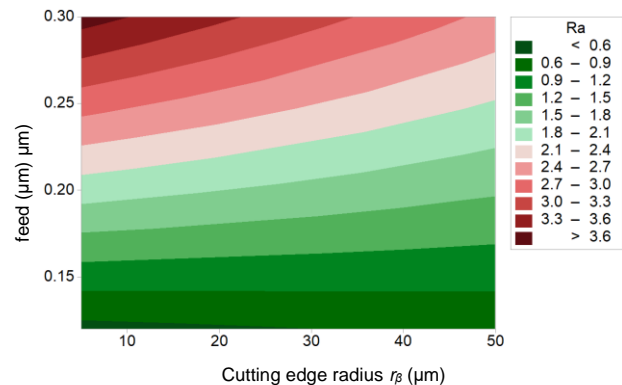


Fig. 11: Contour plot of Ra with respect to the cutting edge radius and feed.

This means that when using low feed values, it is necessary to reduce the ploughing force by using a smaller cutting edge radius, as it can create a significant force component in the resultant force.

On the other hand, when using higher feed values, the resultant force increases, and then a larger cutting edge radius can be used, since the ploughing force represents only a small component of the resultant force. Therefore, surface roughness was not negatively affected by a larger cutting edge radius when higher feed values were used. Moreover, using larger cutting edge radii may be more suitable for challenging machining conditions.

## 5 CONCLUSION

This study examined the influence of cutting edge radius and cutting conditions on surface roughness and microhardness in the turning of austenitic stainless steel (AISI 321).

In case of surface roughness, the study demonstrated that surface roughness parameters Ra and Rz are significantly influenced by the cutting edge radius and feed rate, while cutting speed had no significant effect within the tested range. The results confirm that surface roughness deteriorates with increasing feed, which is attributed to the replication of the tool nose radius on the machined surface, as was generally expected. The analysis of variance (ANOVA) results confirmed the statistical significance of cutting edge radius and feed rate on surface roughness, with interaction effects between these two parameters also playing a critical role. The dependence of surface roughness on cutting edge radius varied with different feed levels. Specifically, at higher feed rates (0.3 mm and 0.2 mm), increasing the cutting edge radius led to a decrease in Ra and Rz, while at a lower feed rate (0.12 mm), the opposite trend was observed. This novel finding suggests a strong correlation between the ratio of uncut chip thickness and cutting edge radius, which influences the strain hardening of the top layer.

In case of microhardness, the study demonstrated that the microhardness of the machined surface is significantly influenced by the cutting edge radius, whereas feed rate and cutting speed had no statistically significant effect. The microhardness of the untreated workpiece material was approximately 280 HV, while the highest microhardness value of 335 HV was observed for a cutting edge radius of 50  $\mu\text{m}$ , indicating a pronounced strain-hardening effect. Conversely, the lowest microhardness value of 282 HV was recorded for a sharp cutting edge (5  $\mu\text{m}$  radius), suggesting minimal plastic deformation in the surface layer. The research confirmed that strain hardening is directly influenced by the position of the separation (stagnation) point, which defines whether the material is sheared into the chip or pressed into the machined surface. The results demonstrated that an increase in cutting edge radius leads to a higher minimum uncut chip thickness, resulting in greater plastic deformation and higher microhardness in the top layer. This effect is evident in the measured microhardness values, where a larger cutting edge radius consistently led to an increase in hardness due to the intensified compressive forces acting below the separation point.

## 6 ACKNOWLEDGMENTS

This research was funded by the EU NextGenerationEU through the Recovery and Resilience Plan for Slovakia under the project No. 09I03-03-V04-00393.

## 7 REFERENCES

- [Boothroyd 2006] Boothroyd, G., and Knight, W. A. *Fundamentals of Machining and Machine Tools*. Taylor and Francis, 2006.
- [Brown 2020] Brown, I., and Schoop, J. The Effect of Cutting Edge Geometry, Nose Radius and Feed on Surface Integrity in Finish Turning of Ti-6Al-4V. *Procedia CIRP*, 87, 2020, pp. 142–147. <https://doi.org/10.1016/J.PROCIR.2020.02.039>.
- [Bushlya 2014] Bushlya, V., Zhou, J., and Ståhl, J. E. Modeling and Experimentation on Multistage Work-Hardening Mechanism in Machining with Nose-Radiused Tools and Its Influence on Machined Subsurface Quality and Tool Wear. *International Journal of Advanced Manufacturing Technology*, 73(1–4), 2014, pp. 545–555. <https://doi.org/10.1007/S00170-014-5837-0/METRICS>.
- [Filippov 2020] Filippov, P., Kaufeld, M., Ebner, M., and Koch, U. Investigation of the Effect of End Mill-Geometry on Roughness and Surface Strain-Hardening of Aluminum Alloy AA6082. *Materials*, 13(14), 2020, p. 3078. <https://doi.org/10.3390/MA13143078>.
- [Hua 2018] Hua, Y., and Liu, Z. Effects of Cutting Parameters and Tool Nose Radius on Surface Roughness and Work Hardening During Dry Turning Inconel 718. *International Journal of Advanced Manufacturing Technology*, 96(5–8), 2018, pp. 2421–2430. <https://doi.org/10.1007/S00170-018-1721-7/METRICS>.
- [Pawade 2008] Pawade, R. S., Joshi, S. S., and Brahmanekar, P. K. Effect of Machining Parameters and Cutting Edge Geometry on Surface Integrity of High-Speed Turned Inconel 718. *International Journal of Machine Tools and Manufacture*, 48(1), 2008, pp. 15–28. <https://doi.org/10.1016/J.IJMACHTOOLS.2007.08.004>.
- [Petropoulos 1973] Petropoulos, P. G. The Effect of Feed Rate and of Tool Nose Radius on the Roughness of Oblique Finish Turned Surfaces. *Wear*, 23(3), 1973, pp. 299–310. [https://doi.org/10.1016/0043-1648\(73\)90019-7](https://doi.org/10.1016/0043-1648(73)90019-7).
- [Rodríguez 2009] Rodríguez, C. *Cutting Edge Preparation of Precision Cutting Tools by Applying Micro-Abrasive Jet Machining and Brushing*. Kassel Univ. Press, 2009; ISBN 9783899587128.
- [Shah 2020] Shah, D., and Bhavsar, S. Effect of Tool Nose Radius and Machining Parameters on Cutting Force, Cutting Temperature and Surface Roughness – An Experimental Study of Ti-6Al-4V (ELI). *Materials Today: Proceedings*, 22, 2020, pp. 1977–1986. <https://doi.org/10.1016/J.MATPR.2020.03.163>.
- [Sharman 2004] Sharman, A. R. C., Hughes, J. I., and Ridgway, K. Workpiece Surface Integrity and Tool Life Issues When Turning Inconel 718TM Nickel-Based Superalloy. *Machining Science and Technology*, 8(3), 2004, pp. 399–414. <https://doi.org/10.1081/MST-200039865>.
- [Vopát 2024] Vopát, T., Kuruc, M., Pätöprstý, B., Vozár, M., Jurina, F., Bočáková, B., et al. The Selection of Cutting Speed to Prevent Deterioration of the Surface in Internal Turning of C45 Steel by Small-Diameter Boring Bars. *Machines*, 12(1), 2024, p. 68. <https://doi.org/10.3390/MACHINES12010068>.
- [Vopat 2020] Vopat, T., Sahul, M., Harsani, M., Vortel, O., and Zlamal, T. The Tool Life and Coating-Substrate Adhesion of AlCrSiN-Coated Carbide Cutting Tools Prepared by LARC with Respect to the Edge Preparation and Surface Finishing. *Micromachines*, 11(2), 2020, p. 166. <https://doi.org/10.3390/MI11020166>.
- [Zhou 2022] Zhou, B., Zhang, W., Gao, Z., and Luo, G. Machining-Induced Work Hardening Behavior of Inconel 718 Considering Edge Geometries. *Materials*, 15(2), 2022, p. 397. <https://doi.org/10.3390/MA15020397>.